Authors response

We thank the anonymous referee for the interest in our study and the careful reading which helped to improve the paper. We hope that our replies to the comments answer the issues in a satisfying way, and that the changes in the manuscript motivated by the comments improved the paper. We first list the central changes in the revised version of the manuscript to give an overview. Then we reply to each comment in a point-by-point response and in the following order: 1.) comment from the reviewer, 2.) our response and 3.) the changes in the manuscript. The modified text passages are given in italics.

Central changes in the revised manuscript:

- We changed the map projection in Fig. 2 from Mercator to Plate Carrée, to match the projection of Fig. 7 (respectively Fig. 6 in the previous version of the manuscript). We furthermore adjusted the colors in Fig. 2 to avoid the combination of red and green filled contours.
- Figure 3 in the revised manuscript now includes information on the occurrence of strong vertical wind shear $S^2 \geq S_t^2$.
- We identified an error in the plotting routine for the latitude-altitude crosssections which depict the temporal and zonally averaged occurrence frequencies for strong vertical wind shear. After a carefull revision of the plotting routine we re-created Fig. 4 and Fig. 5a (Fig. 5b in the revised manuscript). We show the changes here below (Fig. 5 and Fig. 6 in this reply). As can be seen, slightly larger values in the TSL occurrence frequencies are now apparent above the local tropopause. Overall, this revision has no effect on the interpretation of our results and the conclusion of our study.
- Figure 5 now includes an additional panel depicting the zonally averaged occurrence frequencies for strong vertical wind shear in absolute height coordinates (Fig. 5a). It furthermore includes a panel which depicts the zonally averaged occurrence frequencies relative to the cold point tropopause in the tropics respectively relative to the $Q = 2$ pvu dynamic tropopause in the extratropics (Fig. 5c). Both changes were motivated by comments from the two referees.
- The schematic of the averaging method (Fig. 5b in the previous version of the manuscript) is now included as an individual figure (Fig. 6 in the revised manuscript).
- Motivated by a comment from one of the referees we repeated each analysis step concerning the occurrence frequencies of strong vertical wind shear near to the tropopause with an adjusted vertical search range around the LRT to make the results more representative for both the tropics as well as the extratropics. The occurrence of strong vertical wind shear near to the tropopause is now defined as $S^2 \geq S_t^2$ at least within one grid box between 1 km below and 2 km above the LRT. Thus, the occurrence frequencies in Fig. 7, 9, 10, 11, 12 and 13a in the revised manuscript are overall slightly larger

(Fig. 6, 8, 9, 10, 11, 12a in the previous manuscript). This does not affect the interpretation of our results and the overall conclusion of this study.

- The horizontal map projections (Fig. 2, 7 and 12 in the revised manuscript) now depict the horizontal wind on the 200 hPa isobaric surface instead of the vertically integrated horizontal wind (Koch et al., 2006). After revising the manuscript we decided that the vertically integrated wind did not add significant information, and the more commonly depicted horizontal wind on an isobaric surface is more easily to interpret.

- We removed the information on the dynamic tropopause in Fig. 11 in the revised manuscript (Fig. 10 in the previous version) because it was not explicitly discussed in the text.

- Figure 13 in the previous version of the manuscript was replaced by Fig. 14 in the revised manuscript. Figure 14a shows a 2d-histogram of the distribution of N^2-S^2 pairs within the first three kilometers vertical distance from the LRT and for the whole ERA5 data set which is analysed in the study. Figure 14b shows the associated distribution of Richardson numbers in this region. These changes were motivated by comments from the referees.

Point-by-point response to the second review

Main comments:

Comment 1: Generally, the existence of wind shear above the jet core and in the lower stratosphere is not a surprise as is expected from balanced dynamics, the exact structure of the shear zones however are more involved. The authors mention the relation of the shear layer to the thermal wind balance at several instances in the manuscript along with other mechanisms. How much of the structure of the shear layer can be explained by the thermal wind relation? It should be possible to quantify this based on the ERA5 fields. The possible role of gravity waves is mentioned in several sections and maybe this way the magnitude of their contribution could be narrowed down. Furthermore, I would suggest to emphasize more clearly in the introduction, perhaps in a single summarizing sentence, what the main unknown aspects of the shear layer are (e.g. detailed structure, strength, vertical extent and occurrence in a statistical sense, formation mechanism) and which of these aspects are addressed in the study.

Reply to comment 1: We thank the reviewer for this suggestion. We started to compare the wind shear based on the full model wind and the thermal (model) wind. We extended the discussion in Sect. 3 to include a comparison of these two metrics based on a single day analysis (Fig.15 in the manuscript, Fig. 1 in the this reply). The comparison shows that there is in general a good agreement in the larger scale in the extratropics, however, with distinct differences which are presumably mainly caused

by resolved gravity waves. We have not included a climatological analysis of this comparison. We think that such a comparison would increase the content of this manuscript substantially. Also new metrics would need to be introduced, since the metrics used in this study are not suited for such a comparison. The zonal averaging of occurrence frequencies of $S^2 \geq S_t^2$ as well as the quasi-horizontal mapping of strong wind shear near to the tropopause could show a good agreement between actual wind shear and thermal wind shear, even if the thermal wind does not represent the shear regions well, due to a superposition of underestimation and overestimation of the actual wind shear at different longitudes. This is indicated in the exemplary cross sections. We motivate further research on a more general comparison of the TSL with the thermal wind relation at the end of the paragraph.

Concerning the second part of your comment, we have included a more detailed description of the aim of this study at the end of the discussion section.

p.24 L514: The connection between the temperature field and the vertical wind shear for synoptic scale flow can be approximated through the thermal wind relation, i.e., the vertical gradient of the geostrophic wind under the assumption of hydrostatic balance. Figure 14a shows the geostrophic wind at 200 hPa on 11 September 2017, i.e., the date of the exemplary single day analysis in Sect. 3. Overall, the geostrophic wind approximates the synoptic scale flow realistically (compare Fig. 2). However, it overestimates the absolute zonal wind speed in cyclonic rotational systems like the one over the northwest Atlantic, in accordance with the fact that inertial forces are neglected (Holton and Hakim, 2012). The vertical structure of the geostrophic wind is shown exemplarily in the vertical cross sections at 60° *W (Fig. 14b and c). The thermal wind relation results in several regions of strong vertical wind shear near to the tropopause. The comparsion with the vertical wind shear derived from the full model wind reveals a certain degree of agreement, in particular on the synoptic scale, but also differences on the smaller scales. The strength of the vertical wind shear at* 40° *N and 15 km altitude is overestimated by the thermal wind approximation, as well as the shear region directly above that reaches north- and downward. The southward extent of the region of strong wind shear on the other hand is underestimated. The two pronounced wind shear regions below the tropopause and south of* 40° *N are not evident in the the thermal wind shear. The geostrophic zonal wind in the upper troposphere at about* 50° *N deviates from the full model zonal wind, which results in a significant underestimation the vertical wind shear below the tropopause. At the same time, the thermal wind relation overestimates the shear region below the tropopause at* 45° *N, which is caused by strong meridional temperature gradients (not shown). The maximum of the thermal wind shear at* 45° *N directly above the LRT is not evident in the full model wind shear, but instead is apparent in a region that is located further to the north. Overall, the comparison indicates the significance of dynamic processes on smaller scales on which other forces than pressure gradient and Coriolis force need to be taken into account (Newton and Persson, 1962). This example already shows that many details, especially related to mesoscale dynamic features, need to be considered to fully address the differences in the vertical wind shear based on the full model winds and on the thermal wind relation. A comprehensive analysis of these differences is beyond the scope of the current study but will be pursued in future work.*

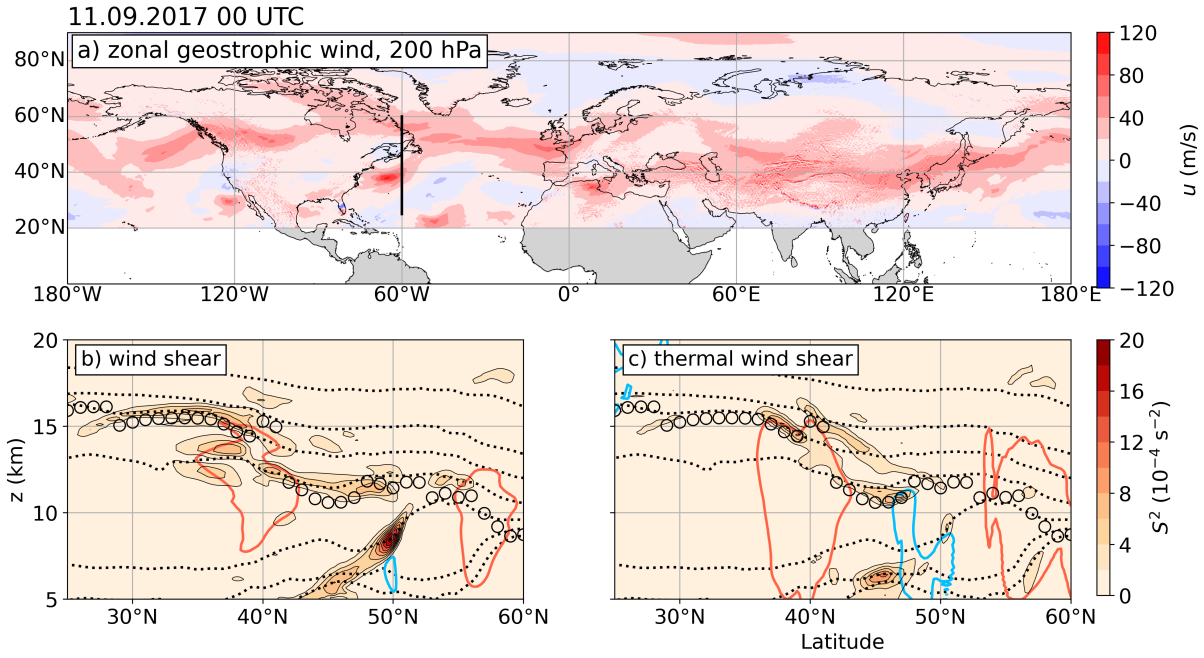

Figure 1. Comparison of the vertical wind shear based on the full model winds and on the thermal wind relation. a) Geostrophic wind at 200 hPa, for the northern hemisphere on 11 September 2017. Regions south of 20° N are left out because the validity of the assumption of geostrophic balance vanishes towards the equator. Black solid line indicates the vertical cross sections in panel b and c. b) Color contour shows vertical shear of the horizontal wind derived from the wind components in the ERA5 data (S^2, in ms^{-2}). Red and blue lines show $u = 30\ \mathrm{ms}^{-1}$ and $u = -10\ \mathrm{ms}^{-1}$ isotachs of the zonal wind. Black dotted lines show isentropes. Black circle markers indicate LRT altitude. c) As in b but for the thermal wind calculated from the temperature field in the ERA5 data. Red and blue lines show $u = 30\ \mathrm{ms}^{-1}$ and $u = -10\ \mathrm{ms}^{-1}$ isotachs of the zonal geostrophic wind.

p.5 L160:This work presents an approach towards such an analysis, on the basis of ten years of northern hemispheric ECMWF ERA5 reanalysis data. The goal is to present a consistent area-wide analysis of the vertical and geographic occurrence frequency distribution for strong wind shear in a state of the art long term numerical representation of the atmosphere, i.e., the ERA5 reanalysis. Compared to observational research studies our approach has no spatial limitiations to assess the occurrence frequency. However, for our analysis it is necessary to keep in mind that the vertical wind shear features are only as well represented as the model resolution allows them to be. An important factor in this context is the vertical resolution, which has improved significantly compared to the ERA-Interim reanalysis as a reference dataset (e.g., Hoffmann et al., 2019). Another important aspect is the choice of the central analysis method, i.e., the analysis of the occurrence frequency distribution of vertical wind shear above a certain threshold value. This approach conserves more information on where strong wind shear occurs in exchange for a loss of information concerning the actual strength of the wind shear, in contrast to the more common

approach of tropopause based averaging.

Comment 2: I think the authors should reconsider some expressions and definitions related to the shear layer phenomenon.
- The words "enhanced" or "exceptional" are used frequently. In what sense is the wind shear "enhanced", compared to what reference? The study shows that the layers of strong wind shear above the tropopause occur rather frequently and strong wind shear is certainly not exceptional near jet streaks.

- The tropopause shear layer (TSL) is defined based on an occurrence frequency criterion. In this sense, it is a purely statistical feature. Since a layer of strong wind shear also seems to be physically present and nicely visible in instantaneous synoptic situations with a strong jet stream (see Fig. 13b), I find it unfortunate to define the "TSL" in a statistical sense rather than as a synoptic feature. It would be more intuitive to call the regions indicated by the red contours in Fig. 13b "TSL".

Reply to comment 2: Concerning the first part of your comment, thank your for pointing that out, we agree that the wording was inconclusive. We changed the wording consistently to “strong vertical wind shear” throughout the manuscript, including the title of the study.

Concerning the second part of your comment, we agree that the choice to define the TSL in such a way is controvertible. However, we wanted to distinguish the individual shear regions from the layer that emerges as an occurrence frequency maximum in the zonal and/or temporal mean. The idea behind the current definition of the TSL was to avoid a definition as to what exactly qualifies as a tropopause wind shear layer in instantaneous wind fields. This concerns for example the horizontal extent, which would raise the question if e.g. a shear region with horizontal extent of the order of 10 km should be defined as a shear layer or rather part of a shear layer. Similarly, this concerns the underlaying forcing mechanism, e.g., does a mesoscale gravity wave perturbation with a sequence of S^2 maxima and minima at the tropopause define individual shear layers or does it rather contribute to the overall occurrence frequency maximum of strong wind shear at the tropopause. We agree with your concern, however, we prefer to keep the current definition of the TSL. We have extended the motivation for the choice of the TSL definition in the manuscript.

p.11 L270: In the following we will refer to the feature of maximum occurrence frequencies at the LRT in the zonal and/or temporal mean as a tropopause shear layer (TSL), however, a comparison with the TIL should be made cautiously. Both features appear similarly in tropopause-relative zonal means (compare with Zhang et al. (2019)), however, the wind shear layer emerges less frequently as well as less area-wide. Furthermore, a different metric is applied here, which analyses the tropopause-relative occurrence frequency of a threshold value S_t^2, instead of directly averaging S^2. We refrain from referring to individual regions of strong wind shear at individual time steps as a tropopause wind shear layer, because this would raise the question of a lower limit for the horizontal and temporal scales that mark such a layer, considering the pronounced mesoscale variability of these regions. We realise that this choice is controvertible, because on a mesoscale horizontal extent of the order of 100 km the geometric aspect ratio between horizontal and vertical extent still clearly describes a layer-like

character.

Comment 3: The authors have chosen a well-considered threshold S_t^2 and the choice is sufficiently explained. However, it would be interesting to test how sensitive the results are with respect to the threshold. How would the pattern of the occurrence frequencies change if S_t^2 was even higher?

Reply to comment 3: We have repeated the analysis concerning the vertical distribution of grid volumes in the different vertical coordinates for a larger threshold value of $S_{t2}^2 = 6 \cdot 10^{-4}\ \mathrm{s}^{-2}$ (Fig. 2 in the present document). While these wind shear values occur significantly less frequently, the LRT-relative averaging still results in the occurrence of a TSL with 10 year temporal and zonal averaged occurrence frequencies of about $1 - 5\ \%$. Overall, the analysis matches the results of the one with $S_t^2 = 4 \cdot 10^{-4}\ \mathrm{s}^{-2}$, with the main difference being generally reduced occurrence frequencies. This applies also to the analysis in the vertical coordinates relative to the CPT and the dynamic tropopause (associated with your comment 4 and comment 3 in the first review). These results are interesting, however, we prefer to not include this analysis in the manuscript, to keep the focus on the threshold that has been motivated in the introduction and the methods section.

Comment 4: I would be curious if the statistical analysis (for the midlatitudes) has also been done relative to the dynamical tropopause and whether there are any differences compared to the LRT-relative framework. This would be interesting e.g. in the context of many STE studies which focus on transport across the 2-PVU surface.

Reply to comment 4: Motivated by his comment and a similar comment by the other referee concerning the cold point tropopause, we repeated the analysis on the vertical occurrence frequency distribution in a vertical coordinate based on the distance of each grid volume from the $Q = 2$ pvu dynmic tropopause in the extratropics (Fig. 2c in the present document, respectively Fig. 5c in the manuscript). We discuss the similarities and differences compared to the LRT-realtive analysis in Sect. 4.1.

p.13 L307: The significance of the processes which result in the occurrence of the TSL remains to be quantified. The clustering of grid volumes which exhibit $S^2 \geq S_t^2$ directly above the LRT in Fig. 5b agrees with the dynamic stability criterion and the thermal wind shear forcing associated with upper tropospheric fronts. However, the overall link between the tropopause definition, which is goverend by the temperature profile, and the occurrence of strong vertical wind shear remains uncertain. Therefore, we repeat the analysis for the tropical cold point tropopause (CPT), i.e., the absolute temperature minimum in the tropical UTLS, and for the dynamic tropopopause, i.e., the $Q = 2$ pvu isosurface in the extratropics. The tropics feature a distinct separation of up to 1 km between the LRT and the CPT (Seidel et al., 2001), which motivates the comparison at low latitudes. The PV on the other hand does not constitute a useful tropopause definition in the tropics (Holton, 1995), which is

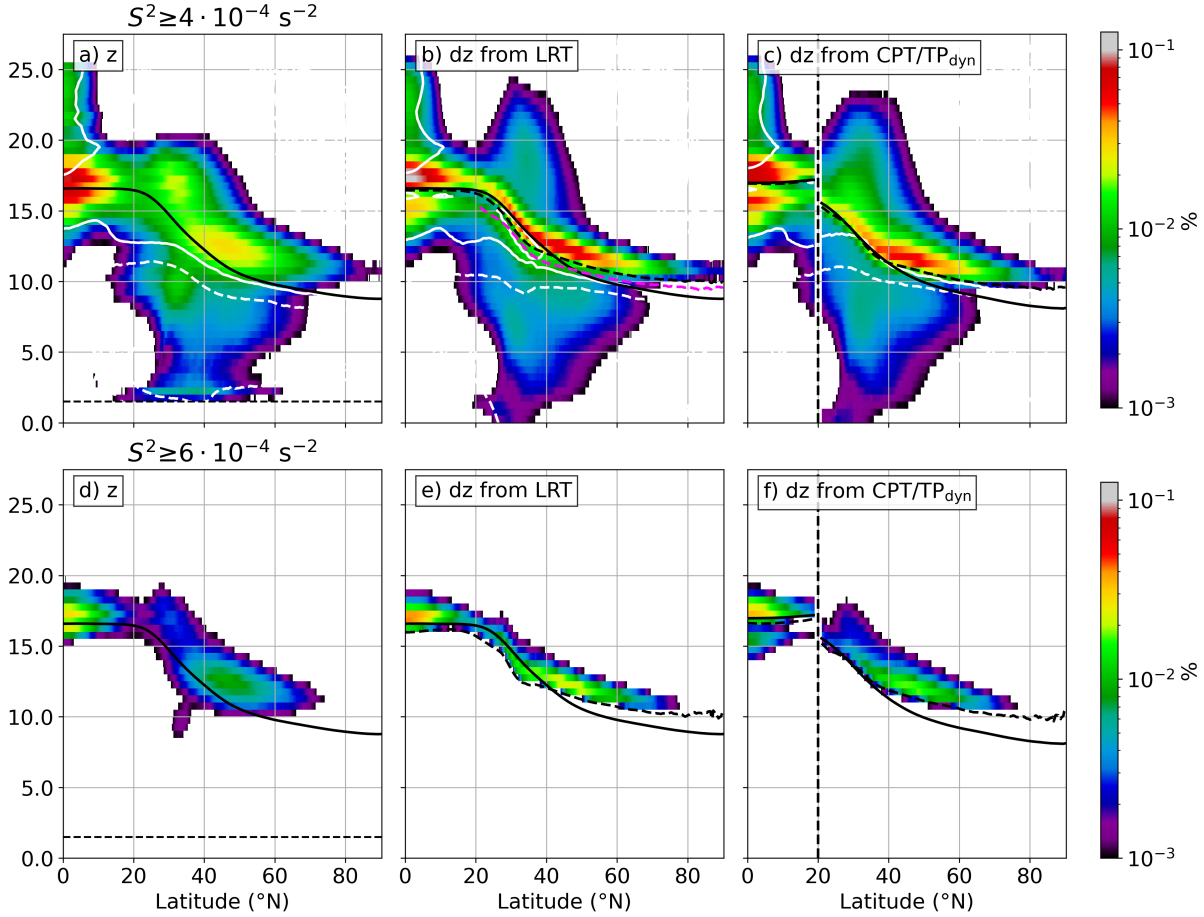

Figure 2. Northern hemispheric occurrence frequency distribution of grid volumes that exhibit strong vertical wind shear $S^2 \geq S_t^2$, from 1 Januaray 2008 to 31 December 2017. Logarithmic frequency contour, vertically binned with $dz = 500$ m. a) Geometric altitude as the vertical coordinate. Solid bold black line indicates mean LRT altitude for all 10 years and the whole northern hemisphere. Dashed thin black line indicates the effect of the 1.5 km above orography cut-off. White solid (dotted) line indicates regions where negative (positive) vertical wind shear makes for 75 % of the counts. b) As in panel a, with LRT-relative vertical coordinate and with mean LRT altitude for profiles with $S^2 \geq S_t^2$ restored (dashed bold black line). Solid bold black line as in panel a. c) As in panel b but from $0° - 20°$ N with the cold point tropopause (CPT) as a reference altitude, and north of $20°$ N with the dynamic tropopause ($Q = 2$ pvu) as a reference altitude. Panels d to e: as in the top column but for $S_{t2}^2 = 6 \cdot 10^{-4}$ s^{-2}.

why the dynamic tropopause is only used in the extratropics in this study. From Fig. 5c it is evident that ERA5 resolves the separation of the LRT and the CPT in the tropics, along with central features like a decreasing mean distance between the two tropopauses towards the equator (Seidel et al., 2001). The clustering of strong wind shear grid volumes above the CPT is less pronounced compared to the LRT, along with a more pronounced secondary maximum below the CPT, which indicates that

the occurrence of strong vertical wind shear is more closely linked to the LRT in the tropics. In the extratropics, the analysis in a vertical coordiante system relative to the dynamic tropopause (Fig. 5c and north of 20° N) compares well with the analysis in the LRT-relative vertical coordinates. At high latitudes, the profiles which exhibit strong vertical wind shear are associated with above average dynamic tropopause altitudes. However, the clustering of grid volumes with $S^2 \geq S_t^2$ above the dynamic tropopause exhibits a larger vertical spread, particularly above the tropopause break. The dynamic tropopause is identified systematically below the LRT in this region, due to the inclusion of PV streamers, as indicated in Fig. 5. Therefore, a larger amount of grid volumes which exhibit strong wind shear are shifted upwards during the averaging process. In conclusion, the averaging of the grid volumes which exhibit $S^2 \geq S_t^2$ based on the distance from the different reference altitudes reveals that the elevation of strong vertical wind shear is (not generally but in the overall mean) more closely linked to the LRT than to the CPT or the dynamic tropopause.

Comment 5: The introduction is quite long, the authors might consider shorten it a bit if possible.

Reply to comment 5: This is a valid point, and we tried to shorten the introduction. However, the information on the subject of strong wind shear in the tropopause region is scattered over a wide range of research studies, which results in the rather extensive introduction section. The following paragraphs have been removed because they did not add relevant information to the introduction. Particularly the third paragraph anticipated results from the analysis sections, and thus, is removed to avoid repitition:

p.3 L69: The results compare well with the ones from Munich, exhibiting a more pronounced averaged vertical wind shear peak during winter, as well as a larger vertical spread compared to summer.

p.3 L84: even though the authors did not make use of a tropopause-relative vertical coordinate.

p.4 L118: This fact, however, is not reflected in the occurrence frequency of reduced Richardson numbers or enhanced turbulence index (TI) values at tropopause altitudes (Jaeger and Sprenger, 2007), which might indicate that the wind shear near to the tropopause is not as pronounced compared to other jet streams. It should, however, be considered that neither the Richardson number nor the TI are solely defined by S^2. The occurrence of a vertical wind shear peak near to the tropopause, as it is apparent in the observational studies, is in fact not necessarily linked to exceptionally large wind speed, because of the limited vertical extent of the shear regions as well as due to the fact that directional shear can contribute to the total wind shear. The summer TEJ presents a descriptive example for this issue. The upper-tropospheric easterlies which define the TEJ exhibit average wind speeds around 40 m/s, which is rather slow compared to the winter STJ and polar jet. They are however associated with the most pronounced near-tropopause maximum in S^2 (Sunilkumar et al., 2015; Zhang et al., 2019)

Specific comments, suggestions and typos:

Comment: L13ff: Throughout the manuscript, the term "tropopause-based" vertical wind shear is used frequently. This expression is not very clear to me; does it mean "tropopauserelative", "near-tropopause" or "tropopause-level"?).

Reply to comment: We agree and changed the wording consistently to “strong vertical wind shear near to the tropopause”.

Comment: L30: an –> a

Reply to comment: Done.

Comment: L36: to the –> its

Reply to comment: Done.

Comment: L60 and all following occurrences: ° N –> °N, please remove the space between "°" and "N"/"E"/"S"/"W"

Reply to comment: The WCD guidelines state that “coordinates need a degree sign and a space when naming the direction (e.g. 30° N, 25° E).”

Comment: L61: for –> of

Reply to comment: Done.

Comment: L67: ERA Interim –> ERA-Interim

Reply to comment: Done, and in one other instance. Thank you for pointing that out.

Comment: L67: data set –> dataset

Reply to comment: Done.

Comment: L70: remove "on"

Reply to comment: Done.

Comment: L93: data –> forecasts

Reply to comment: Done.

Comment: L98: analysis data –> analyses

Reply to comment: Kaluza et al. (2019) use operational analysis data from the ECMWF IFS.

Comment: L105: presents –> constitutes

Reply to comment: Done, good suggestion.

Comment: L109: causes –> cause

Reply to comment: Done.

Comment: L173: analysis "of" a single day

Reply to comment: Done.

Comment: L174: Sections –> Section

Reply to comment: Done.

Comment: L178: Please check the date and time convections of WCD

Reply to comment: The WCD guidelines state: “Date and time: 25 July 2007 (dd month yyyy)”. We now use this convention consitently throughout the manuscript.

Comment: L185: ERA5 provides omega in Pa/s, not w in m/s

Reply to comment: Thank your for pointing that out. We changed the variable name accordingly.

Comment: L189: dynamic –> dynamical

Reply to comment: Done.

Comment: L191: Please remove the symbol for the cross product and insert a comma after equation. / L192: (with the angular velocity of the Earth, Omega).

Reply to comment: Done.

p.6 L191: Following the definition of Ertel (1942) the potential vorticity (PV) can be written as

$$Q = \frac{1}{\rho}\boldsymbol{\eta} \cdot \boldsymbol{\nabla}\Theta, \tag{1}$$

where ρ is the density of the medium, and $\boldsymbol{\eta} = \boldsymbol{\nabla} \times \boldsymbol{u} + 2\boldsymbol{\Omega}$ the vector of the absolute vorticity with the angular velocity of the earth $\boldsymbol{\Omega}$.

Comment: L196: How do you derive the vertical distance between the model levels, do you use geopotential?

Reply to comment: That is correct. We have added the according information in the methods description

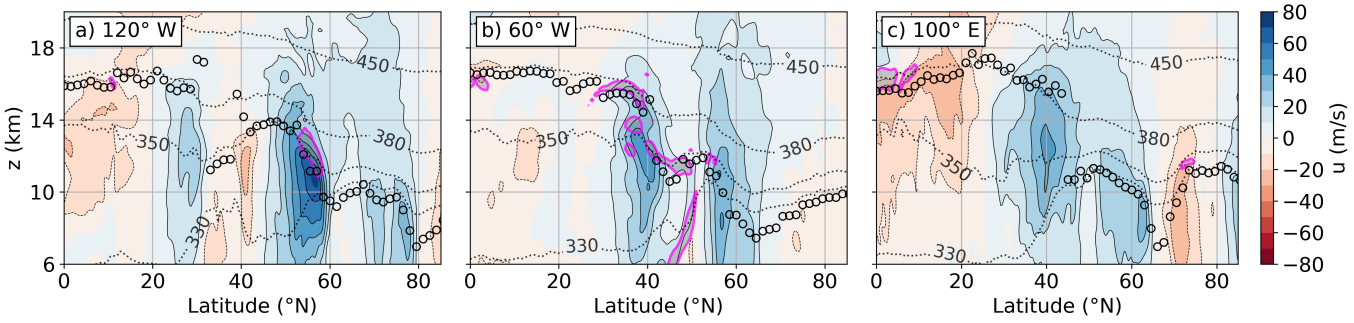

Figure 3. Vertical cross sections on 11 September 2017, at 00 UTC and at a) 120° W, b) 60° W, and c) 100° E. Colour contour shows zonal wind speed (u, in $\mathrm{m\ s^{-1}}$), black dots LRT altitude, and black dotted lines isentropes (Θ, in K). Magenta lines show $S^2 = S_t^2$ isolines.

p.7 L203: The altitude at each model level is derived from the geopotential after vertically integrating the hydrostatic equation from the pressure and temperature profiles (for further information refer to the IFS documentation, ECMWF (2016)).

Comment: L201: can not –> cannot

Reply to comment: Done.

Comment: L202: for –> to

Reply to comment: Done.

Comment: L203: It is a bit confusing to read about static stability in combination with the notation S_t^2.

Reply to comment: Thank your for pointing that out, it was a typo.

Comment: L209: majorly –> mostly

Reply to comment: Done.

Comment: Fig3: It would be interesting to see contours of S^2 in the snapshot vertical cross sections in addition to wind speed. This would illustrate not only the general position of the shear zones but also the spatial variability.

Reply to comment: We have included isolines that indicate the location of $S^2 = S_t^2$ in the vertical cross sections (Fig. 3 in the present document, Fig. 3 in the manuscript). We furthermore replaced the cross section in Fig. 3b with the cross section at 60° W, which was previously shown in Fig. 13b. Thus, the cross section is not implemented twice.

Comment: L259-264: Here, it would be helpful to explicitly point out the different positions of the solid/dashed black lines in Fig. 5a.

Reply to comment: We agree, and we have now pointed out the different tropopause averages and the according lines in Fig. 5 in the paragraph that discusses the vertical cross sections. Furthermore, the depiction of the different tropopause averages is now more consistent throughout the manuscript (Fig. 4, 5 and 11)

Comment: L267-270: While the schematic illustration in Fig. 5b is very helpful and easy to understand, I find the explanation in the text rather unclear. The authors might consider rewriting these sentences.

Reply to comment: We extended the description of the averaging effect that results in the large spread of the secondary occurrence frequency maxima above and below the tropopause break.

p.12 L288: Furthermore, an enhanced vertical spread of $S^2 \geq S_t^2$ is apparent at the tropopause break in the LRT-relative vertical coordinates (Fig. 5b) compared to the geometric altitude (Fig. 5a). Figure 6 illustrates how this can be explained by the averaging method. Below the jet core of the STJ strong vertical wind shear occurs frequently within PV streamers (Škerlak et al., 2015), i.e., tounges of stratospheric air that reach south- and downward. They are characterised by stratospheric PV values, which is linked to the frontal character of the inherent temperature gradients. The horizontal temperature gradients are associated with a strong thermal wind forcing, and the resulting vertical wind shear can be sustained by the vertical temperature gradients. Despite the stratospheric characteristics of these air masses, the LRT criterion which requires a mean lapse rate below 2.0 K km^{-1} over a vertical distance of 2 km is no longer met at some point within the PV streamers, which is indicated by the dashed black line in Fig. 6. In these cases the LRT is located at the upper edge the tropopause break and several kilometers above the region of strong wind shear. Eventually, the 10 year temporally and zonally averaged LRT altitude exhibits a more smooth transition between the lower and the upper edge of the tropopause break (right panel in Fig. 6), which is caused by short-period as well as seasonal meandering of the tropopause break. The LRT-relative averaging method ultimately shifts the region of strong wind shear downward from the mean LRT altitude, over the distance which was originally determined relative to the instantaneous LRT. The equivalent effect also occurs at the upper edge of the tropopause break as indicated in Fig. 6.

Comment: L298: barclinic –> baroclinic

Reply to comment: Done.

Comment: L315-316: I assume your background state is still latitude-dependent? From this sentence it is not clear if you also average over latitudes.

Reply to comment: This information is now explicitly stated.

p.15 L371: We preserve the meridional dependency and define the zonal and temporal average $\overline{\Theta}(Q = 2\ \mathrm{pvu})$ in the meridional region from 35° N–60° N as the background state for the following analysis.

Comment: Fig7a: What does the black dot indicate?

Reply to comment: The black dot indicates $\overline{\Theta}(Q = 2\ \mathrm{pvu})$ at 51° N and during SON over the Atlantic region, i.e., the mean potential temperature that defines the background state for the analysis in Fig. 9. This information was missing in the caption of Fig. 7 and is now included.

Comment: L326: Why did you choose exactly 51°N?

Reply to comment: To some extent the choice is arbitrary, the primary intention was to introduce the metric. According to Fig. 10a the occurrence frequencies maximise at these latitudes. Thus, the choice represent a descriptive example.

Comment: L355: DFJ –> DJF

Reply to comment: Done.

Comment: L416: and "references" therein

Reply to comment: Done.

Comment: L440-441: No co-location of TIL and TSL: Can you show this in a figure? Maybe a snapshot vertical cross section would do. Or perhaps something like a frequency distribution of N^2 in the lowest 2 km above the LRT, showing grid cells with $S^2 \geq S_t^2$ separately and comparing them to the N^2 distribution of all grid cells.

Reply to comment: We agree that this statement concerning the non-correlation of N^2 and S^2 needs to be substantiated. The discussion section now includes such a 2d-histogram (Fig 4a in the present document, Fig. 14a in the manuscript), along with the according discussion. This figure is also used in the subsequent discussion on the occurrence of comparatively low Richardson numbers in the lower stratosphere.

p.23 L499: Figure 14a shows the relative occurrence frequency of N^2-S^2 pairs for all ten years and in the region between the LRT and 3 km above. The majority of grid volumes exhibit a static stability between the stratospheric background $\overline{N^2}_{strat.} = 4 \cdot 10^{-4}\ \mathrm{s}^{-2}$ and moderately enhanced values associated with the TIL. At the same time, comparatively "weak" vertical wind shear $S^2 < 4 \cdot 10^{-4}\ \mathrm{s}^{-2}$ is most prevalent. Vertical wind shear and static stability do not correlate, and enhanced values of S^2 can be found within a large spectrum of N^2 under the condition that dynamic stability $Ri > Ri_c$ is (for the most part) maintained. Particularly the largest values of N^2 and S^2 do not correlate.

Comment: L449-453: Are gravity waves (partially) resolved in ERA5?

Reply to comment: The other referee pointed out two recent research studies on that matter, which are now cited in the discussion section. Central features of the gravity wave spectrum are in fact resolved in the ERA5 reanalysis.

p.24 L539: Recently, Podglajen et al. (2020) compared long-duration superpressure balloon measurements with Lagrangian trajectories calculated from a set of numerical reanalysis products, and where able to show that the ERA5 reanalysis resolves

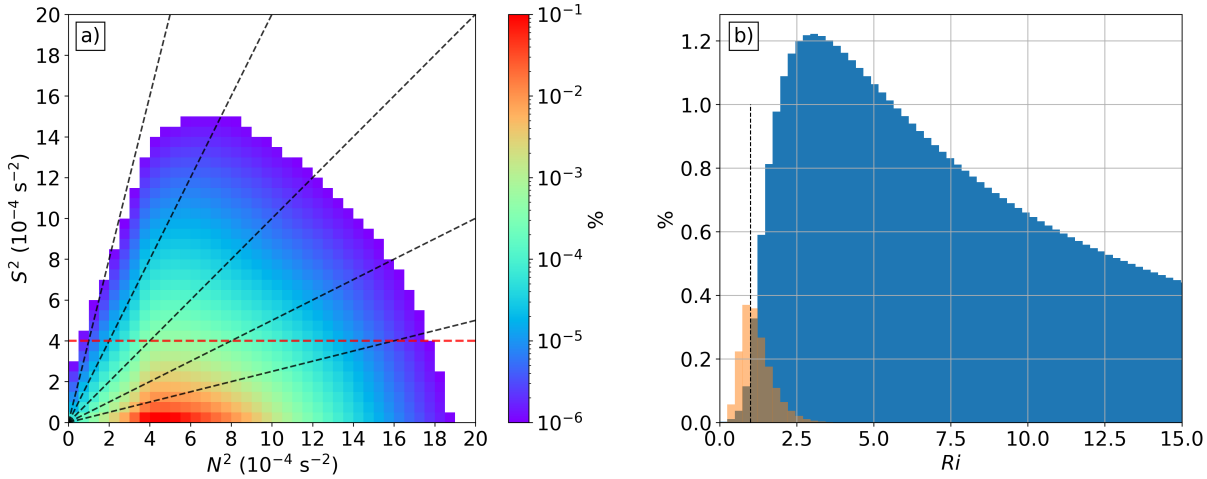

Figure 4. a) Relative occurrence frequency distribution of N^2-S^2 pairs in the region between the LRT and 3 km above, for all daily northern hemispheric ERA5 fields from 2008-2017. Logarithmic occurrence frequency color scale. Red dashed line indicates $S^2 = S_t^2$. Dashed black lines indicate the Richardson numbers 0.25, 0.5, 1.0 ,2.0 and 4.0. b) Histogram of the relative distribution of Richardson numbers associated with the data displayed in panel a. Orange bars show Ri for grid volumes with $S^2 \geq S_t^2$, and blue bars for the remaining grid volumes between the LRT and 3 km above. Dotted black line indicates $Ri = 1$.

central features of the gravity wave spectrum. The underlaying IFS model resolves low frequency large scale gravity waves down to wavelengths which approach the effective resolution, which is generally estimated to exhibit a factor of about 10 compared to the effective grid spacing. The assimilation of high resolution observational data further enhances the gravity wave activity in the model, which likely involves generation processes and gravity wave scales that are not resolved in the IFS. Furthermore, Krisch et al. (2020) identified individual wave packets in the ERA5 data that had been observed with the Gimballed Limb Observer for Radiance Imaging of the Atmosphere (GLORIA) during the GW-LCYCLE airborne measurement campaign. While these studies confirm that modern reanalysis products are capable to resolve central features of the gravity wave spectrum, the overall vertical wind variability due to gravity waves is likely still underestimated in the ERA5. Recently, Schäfler et al. (2020) reported a significant underestimation of the vertical wind shear near to the tropopause in the IFS, based on a comparison of Doppler wind lidar measurements with IFS analysis and forecast data. The analysis and forecast errors were most prominent at elevated tropopause altitudes above upper tropospheric ridges, i.e., regions that contribute significantly to the occurrence of the TSL in the extratropics. To put these results into context, the model version used by Schäfler et al. (2020) exhibits a spectral truncation of TCo1280 on 137 vertical level, thus, the same vertical grid spacing compared to the ERA5 as well as a larger horizontal resolution.

Comment: Fig13b: Do the black circles indicate the LRT?

Reply to comment: That is correct. This cross section and the according description is now implemented in Fig. 3b in the manuscript (Fig. 3b in the present document).

Comment: L487: I believe that throughout the summary the expressions "exceptionally pronounced/strong/enhanced vertical wind shear" and "enhanced tropopause-based vertical wind shear" are used synonymously. Perhaps consider using the same formulation throughout the paper (including introduction) to not confuse the reader.

Reply to comment: Thank you for pointing that out, we agree that the inconsistency is confusing to the reader. We changed the wording, and now refer to $S^2 \geq S_t^2$ as “strong vertical wind shear”, which includes the title of the study.

Comment: L528: dynamic –> dynamical

Reply to comment: Done.

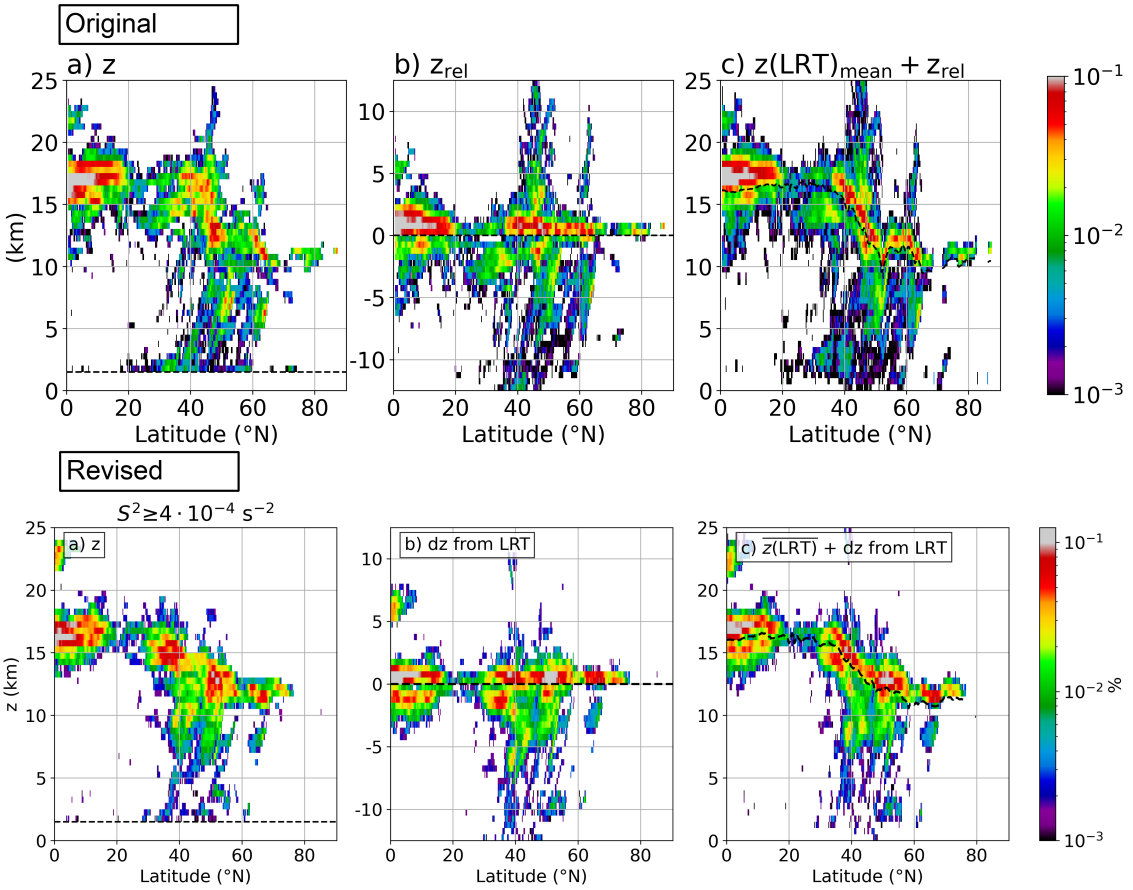

Figure 5. Comparison of Fig. 4 in the originally uploaded manuscript (top row) and the equivalent in the revised manuscript (bottom row). The colorbars had to be extended slightly at the top end due to the larger maximum values, however, with the same colors in the frequency range of $10^{-3} - 10^{-1}$.

References

ECMWF: IFS documentation – Cy41r2 Operational implementation 8 March 2016 Part III : Dynamics and numerical procedures, in: IFS Documentation CY41R2, ECMWF, https://doi.org/10.21957/83wouv80, 2016.

Ertel, H.: Ein neuer hydrodynamischer Erhaltungssatz, Die Naturwissenschaften, 30, 543–544, https://doi.org/10.1007/BF01475602, 1942.

Hoffmann, L., Günther, G., Li, D., Stein, O., Wu, X., Griessbach, S., Heng, Y., Konopka, P., Müller, R., Vogel, B., and Wright, J. S.: From ERA-Interim to ERA5: The considerable impact of ECMWF's next-generation reanalysis on Lagrangian transport simulations, Atmospheric Chemistry and Physics, 19, 3097–3214, https://doi.org/10.5194/acp-19-3097-2019, 2019.

Holton, J. R.: Stratosphere–Troposphere Exchange, Stratosphere Troposphere Interactions, pp. 331–355, https://doi.org/10.1007/978-1-4020-8217-7_8, 1995.

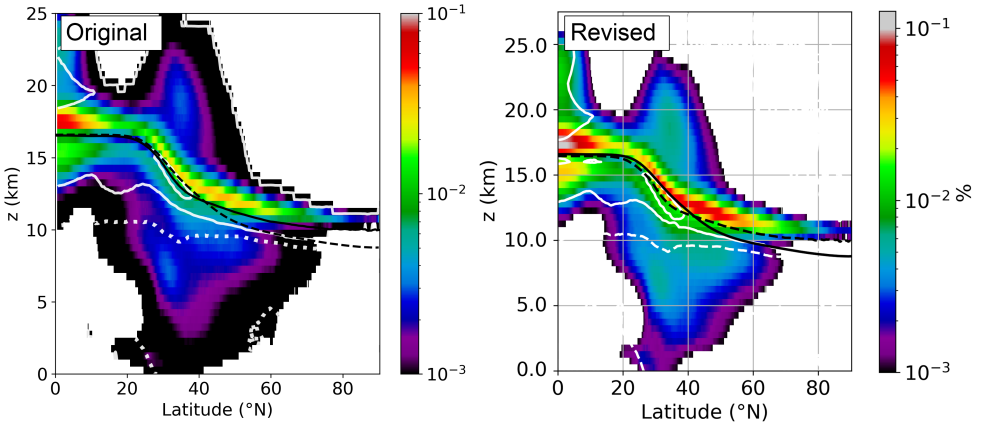

Figure 6. Comparison of Fig. 5a in the originally uploaded manuscript (left panel) and the equivalent in the revised manuscript (right panel). The colorbars had to be extended slightly at the top end due to the larger maximum values, however, with the same colors in the frequency range of $10^{-3} - 10^{-1}$.

Holton, J. R. and Hakim, G. J.: An introduction to dynamic meteorology: Fourth edition, vol. 9780123848, Elsevier, fourth edi edn., https://doi.org/10.1016/C2009-0-63394-8, 2012.

Jaeger, E. B. and Sprenger, M.: A Northern Hemispheric climatology of indices for clear air turbulence in the tropopause region derived from ERA40 reanalysis data, Journal of Geophysical Research Atmospheres, 112, 1–13, https://doi.org/10.1029/2006JD008189, 2007.

Kaluza, T., Kunkel, D., and Hoor, P.: Composite analysis of the tropopause inversion layer in extratropical baroclinic waves, Atmospheric Chemistry and Physics, 19, 1–22, https://doi.org/10.5194/acphttps://doi.org/10.5194/acp-19-6621-2019-2018-1100, 2019.

Koch, P., Wernli, H., and Davies, H. C.: An event-based jet-stream climatology and typology, International Journal of Climatology, 26, 283–301, https://doi.org/10.1002/joc.1255, 2006.

Krisch, I., Ern, M., Hoffmann, L., Preusse, P., Strube, C., Ungermann, J., Woiwode, W., and Riese, M.: Superposition of gravity waves with different propagation characteristics observed by airborne and space-borne infrared sounders, Atmospheric Chemistry and Physics, 20, 11 469–11 490, https://doi.org/10.5194/acp-20-11469-2020, 2020.

Newton, C. W. and Persson, A. V.: Structural characteristics of the subtropical jet stream and certain lower-stratospheric wind systems, Tellus, 14, 2, https://doi.org/10.3402/tellusa.v14i2.9542, 1962.

Podglajen, A., Hertzog, A., Plougonven, R., and Legras, B.: Lagrangian gravity wave spectra in the lower stratosphere of current (re)analyses, Atmospheric Chemistry and Physics, 20, 9331–9350, https://doi.org/10.5194/acp-20-9331-2020, 2020.

Schäfler, A., Harvey, B., Methven, J., Doyle, J. D., Rahm, S., Reitebuch, O., Weiler, F., and Witschas, B.: Observation of jet stream winds during nawdex and characterization of systematic meteorological analysis errors, Monthly Weather Review, 148, 2889–2907, https://doi.org/10.1175/MWR-D-19-0229.1, 2020.

Seidel, D. J., Ross, R. J., Angell, J. K., and Reid, G. C.: Climatological characteristics of the tropical tropopause as revealed by radiosondes, Journal of Geophysical Research Atmospheres, 106, 7857–7878, https://doi.org/10.1029/2000JD900837, 2001.

Škerlak, B., Sprenger, M., Pfahl, S., Tyrlis, E., and Wernli, H.: Tropopause folds in ERA-interim: Global climatology and relation to extreme weather events, Journal of Geophysical Research, 120, 4860–4877, https://doi.org/10.1002/2014JD022787, 2015.

Sunilkumar, S. V., Muhsin, M., Parameswaran, K., Venkat Ratnam, M., Ramkumar, G., Rajeev, K., Krishna Murthy, B. V., Sambhu Namboodiri, K. V., Subrahmanyam, K. V., Kishore Kumar, K., and Shankar Das, S.: Characteristics of turbulence in the troposphere and lower stratosphere over the Indian Peninsula, Journal of Atmospheric and Solar-Terrestrial Physics, 133, 36–53, https://doi.org/10.1016/j.jastp.2015.07.015, 2015.

Zhang, Y., Zhang, S., Huang, C., Huang, K., and Gong, Y.: The Tropopause Inversion Layer Interaction With the Inertial Gravity Wave Activities and Its Latitudinal Variability, Journal of Geophysical Research: Atmospheres, 124, 7512–7522, https://doi.org/10.1029/2019JD030309, 2019.